

Responses of coral reef community metabolism in flumes to ocean acidification

R. C. Carpenter¹ · C. A. Lantz^{1,2} · E. Shaw¹ · P. J. Edmunds¹

Received: 4 June 2017 / Accepted: 8 March 2018 / Published online: 17 March 2018
© Springer-Verlag GmbH Germany, part of Springer Nature 2018

Abstract

Much of the research on the effects of ocean acidification on tropical coral reefs has focused on the calcification rates of individual coral colonies, and less attention has been given to carbonate production and dissolution at the community scale. Using flumes ($5.0 \times 0.3 \times 0.3$ m) located outdoors in Moorea, French Polynesia, we assembled local back reef communities with $\sim 25\%$ coral cover, and tested their response to pCO_2 levels of 344, 633, 870 and 1146 μatm . Incubations began in late Austral spring (November 2015), and net community calcification (G_{net}) and net community primary production (P_{net}) were measured prior to treatments, 24 h after treatment began, and biweekly or monthly thereafter until early Austral autumn (March 2016). G_{net} was depressed under elevated pCO_2 over 4 months, although the magnitude of the response varied over time. The proportional decline in G_{net} as a function of saturation state of aragonite (Ω_{ar}) depended on the initial Ω_{ar} , but was 24% for a decline in Ω_{ar} from 4.0 to 3.0, which is nearly twice as sensitive to variation in Ω_{ar} than the previously published values for the net calcification of ex situ coral colonies. However, community G_{net} was less sensitive to Ω_{ar} than coral reefs that have been analyzed in situ. P_{net} was unaffected by pCO_2 , but P_{net} and G_{net} expressed on a hourly time base were positively associated, thus revealing the tight coupling between these metabolic processes. The high sensitivity of G_{net} to pCO_2 for the back reef of Moorea, versus lower sensitivity of individual coral colony calcification to pCO_2 , underscores the challenges of scaling-up experimental results on the effects of pCO_2 from coral reef organisms to coral reef communities.

Introduction

Coral reefs are one of the most vulnerable ecosystems to ocean acidification (Kleypas and Yates 2009), which is the product of increasing anthropogenic carbon dioxide (CO_2) emissions, and the dissolution of CO_2 in seawater. The dissolution of CO_2 into the surface ocean elevates the aqueous

partial pressure of CO_2 (pCO_2), thereby decreasing seawater pH and the saturation state (Ω) of calcium carbonate [CaCO_3 as aragonite (Ω_{ar}) and calcite (Ω_{ca})] without affecting total alkalinity (A_{T}) (Doney et al. 2009). It is widely recognized that these effects will decrease the rates at which many coral reef calcifiers deposit CaCO_3 (Kroeker et al. 2013; Comeau et al. 2014a), and increase the CaCO_3 dissolution of reef communities (Andersson and Gledhill 2013; Eyre et al. 2014; Comeau et al. 2016). Combined, these trends are expected to cause community net calcification (G_{net} , gross calcification minus dissolution) to decline on coral reefs, and potentially degrade structural habitat complexity that is formed through biogenic calcification (Hoegh-Guldberg et al. 2007; Comeau et al. 2016).

In situ measurements of coral reef community G_{net} have shown that it is affected by natural diel variations in seawater carbonate chemistry (Shaw et al. 2012). For example,

G_{net} was associated significantly ($r^2=0.33$) with diurnal variation in Ω_{ar} (with a median diurnal variation of 3.25) at Lady Elliot Island, Australia (Shaw et al. 2012). Based on field measurements of the relationships between Ω_{ar} and G_{net} , Silverman et al. (2009) predicted that coral reefs would

Responsible Editor: R. Hill.

Reviewed by T. DeCarlo and undisclosed experts.

Electronic supplementary material The online version of this article (<https://doi.org/10.1007/s00227-018-3324-0>) contains supplementary material, which is available to authorized users.

✉ R. C. Carpenter
robert.carpenter@csun.edu

¹ Department of Biology, California State University, 18111 Nordhoff Street, Northridge, CA 91330-8303, USA

² School of Environmental Science and Engineering, Southern Cross University, Military Road, East Lismore, NSW 2480, Australia

transition from net calcification to net dissolution at 560 ppm atmospheric pCO₂, which potentially could occur within 50 years (IPCC, 2014). However, for scleractinian corals that are the ecosystem engineers of coral reefs (Jones et al. 1994; Wild et al. 2011) and a major contributor to their CaCO₃ production (Perry et al. 2013), there is interspecific variation in the sensitivity of calcification to increases in pCO₂ (Chan and Connolly 2013; Comeau et al. 2014a). The calcification rates of many species are affected strongly and negatively by high pCO₂ (Chan and Connolly 2013; Comeau et al. 2014a), but in some species, they are affected less severely (Comeau et al. 2014a). The sensitivity of calcification to pCO₂ can be both species and life history stage specific and related to the extent to which organisms are able to biologically control the calcification process (Comeau et al. 2014a). Generally, net calcification of individual coral species appears to be less sensitive to elevated pCO₂ than it is for the coral reef communities they build (Pandolfi et al. 2011; Comeau et al. 2015; 2016).

It is unknown, however, whether the greater sensitivity of coral reef community G_{net} to ocean acidification, relative to coral colonies, reflects methodological artifacts, or is the result of emergent properties of the communities, for example, the propensity of some of their inorganic components for dissolution (Andersson and Gledhill 2013; Eyre et al. 2014). Unlike the laboratory experiments that typically are employed to study the response of corals to elevated pCO₂, when *in situ* approaches are used to evaluate the relationship between community G_{net} for coral reefs and pCO₂, it is difficult methodologically to control seawater pCO₂ or pH precisely to simulate future conditions (although see Albright et al. 2016). The other conditions that are likely to covary with pCO₂ include light availability, seawater temperature, nutrient concentrations, and flow regimes, all of which could affect the response of community G_{net} to seawater carbonate chemistry (Comeau et al. 2014b). The quality and quantity of light, for example, affects community net photosynthesis (P_{net}) on coral reefs, which is a driver of community G_{net} (Kinsey 1985; Falter et al. 2008), but community P_{net} also affects seawater carbonate chemistry through the uptake of dissolved inorganic carbon [(DIC), Anthony et al. 2008b; Shaw et al. 2012]. Together, these effects cause community G_{net} to be associated with seawater carbonate chemistry, light availability, and community P_{net} (Falter et al. 2012).

Rates of primary production on coral reefs primarily are driven by light availability, but they can be modified by additional factors such as temperature, nutrient availability, and water flow (Dennison and Barnes 1988; Atkinson et al. 1999; Langdon and Atkinson 2005). P_{net} and G_{net} typically are associated strongly for both organisms and communities on minute-to-hourly time scales, in part because photosynthesis provides fixed carbon that can be used to supply metabolic energy supporting the costs of calcification (Allemand

et al. 2011; Frieder et al. 2016), and it can also create a pH environment favoring calcium carbonate deposition (Allemand et al. 2011). For coral reefs, evidence that ocean acidification affects P_{net} at any level of biological organization is equivocal (Anthony et al. 2008a; Crawley et al. 2010; Dove et al. 2013; Comeau et al. 2016); however, the relationship between community P_{net} and G_{net} can be altered by ocean acidification (DeCarlo et al. 2017), reflecting a disruption of the coupling between organic and inorganic carbon fixation.

In situ analyses of coral reef community metabolism (i.e., G_{net} and P_{net}) typically use short experiments in which measurements employing the alkalinity anomaly techniques (Kinsey 1978; Smith and Kinsey 1978) are completed over minutes-to-days (Gattuso et al. 1996; Shaw et al. 2015; DeCarlo et al. 2017). This resolution reflects the need to constrain some experimental work to periods with reduced seawater flow (e.g., slack water), but it also is important to detect rapid changes in community G_{net} , such as how it occurs in response to diel variation in carbonate chemistry (Ohde and van Woesik 1999; Shaw et al. 2012). Other approaches (e.g., Lagrangian transects) quantify metabolic rates over one to several days (e.g., Kinsey 1985; Gattuso et al. 1996). To date, however, there is limited evidence of the extent to which short-term experiments and measurements are indicative of responses occurring over months-to-years (Kroeker et al. 2013). The present study is part of a larger project to measure the metabolic response of coral reef communities to elevated pCO₂ over ecologically relevant time scales, and here we present the results from the first 4 months of this experiment. Working with a benthic community from the back reef of Moorea, French Polynesia, we present the results of an experiment in which we measured community G_{net} and P_{net} under four pCO₂ regimes from late Austral spring to early Austral autumn. Using community G_{net} and P_{net} as dependent variables, we tested the hypothesis that the effects of pCO₂ are consistent over times-scales ranging from 1 day to 4 months. As a means to test our hypothesis, we also explored the effects of pCO₂ on diel variation in community G_{net} and P_{net} as well as the degree to which these variables were associated.

Methods

Coral reef communities were assembled in four, outdoor flumes in Moorea, French Polynesia. Logistical constraints of constructing, instrumenting, and maintaining additional flumes precluded an experimental design with replicate flumes for each pCO₂ treatment. Instead of using a factorial experimental design, we employed a regression approach to explore the community level responses to increasing pCO₂, and to evaluate whether those responses varied over time. Each flume was assigned randomly seawater carbonate

chemistry conditions created by four pCO_2 regimes, targeted at ambient (400 μatm), 700, 1000 and 1300 μatm pCO_2 , and treatments were maintained for 4 months from late Austral spring (November 2015) to early Austral autumn (March 2016); actual pCO_2 treatments differed slightly from target values (described below). The working section of each flume was filled to 30-cm depth with seawater, and the communities were assembled in each of the 5.0 m \times 0.3 m working sections. The flumes (described in Comeau et al. 2015) contained \sim 500 L of seawater that was circulated continually and augmented with fresh seawater at \sim 5 L min^{-1} . Seawater was pumped from 14-m depth in Cook's Bay, and filtered through sand (nominal pore size 450–550 μm) prior to flowing into the flumes. This effectively allowed smaller particles to enter the flume and serve as a potential food source for heterotrophic organisms.

Preparation of back reef communities in flumes

Coral reef communities were assembled to correspond to the mean percent cover of the major benthic space holders on the back reef of Moorea in 2013 (Fig. S1) (Carpenter 2016a; Edmunds 2016) and the communities were similar to those we have tested previously for response to elevated pCO_2 over shorter periods (\leq 56 days) (Comeau et al. 2014b; 2015). Each flume contained \sim 25% coral cover, comprised of 11% cover of massive *Porites* spp., 7% *Porites rus*, 4% *Montipora* spp. and 3% *Pocillopora* spp. There was \sim 7% cover of crustose coralline algae (CCA), with 4% *Porolithon onkodes* and 3% *Lithophyllum kotschyannum*, and \sim 5% cover of small pieces (i.e., \sim 1-cm diameter) of coral rubble (Fig. S2).

The working section of each flume included a 2.4-m long sediment chamber that extended the width of the flume, and contained 30-cm depth of sand collected from the back reef. The sediment chamber was in the center of the working section of the flume, and was flanked on either end by 1.3 m of the fiberglass floor of the flume. In addition to the live coral, sand, CCA, and rubble, the flumes also included three small holothurians (\sim 8-cm long, *Holothuria leucospilota*), and thalli of the macroalgae *Turbinaria ornata* and *Halimeda minima* to approximate the cover of these algae in the back reef in 2013. The cover of these algae, therefore, were targeted at 11 and 1% (respectively), but the necessity of replacing them consistently throughout the incubation resulted in periodic and substantial downward variability in macroalgal cover in each flume. As the objective was to create ecologically relevant back reef communities, and expose them for multiple months to treatment conditions, the communities were not standardized for the abundances of small (i.e., \leq 1-cm diameter) taxa associated with coral reef communities. We rationalized this approach by the large size of the flume communities, the strong likelihood that effectively they sampled the same community from which they were

collected, and the difficulty of ensuring that 1.2 m² areas (and sediments to 30-cm depth) of experimental reef were identical biologically.

Corals, CCA, and rubble were collected from <2 -m depth in the back reef of Moorea. After collection, corals and CCA were epoxied to plastic bases, and placed in a seawater table for 3 days before being installed in the flumes under ambient seawater carbonate chemistry conditions. Sediments were collected from the back reef at \sim 2-m depth, and were placed into plastic sediment boxes (0.4 \times 0.3 \times 0.3 m) that were left in situ (i.e., buried in sand with their upper surface at the natural sand level) for 3 days to promote natural sediment stratification (after Comeau et al. 2015). The sediment boxes then were inserted into the flume in the same vertical orientation to maintain sediment stratification. Reef communities were assembled in the flumes on 12 November 2015, and were maintained under ambient conditions for 5 days (until 17 November), when treatment pCO_2 levels were applied to three randomly selected flumes (the fourth remained at ambient pCO_2). Stable treatment levels were established within a 24-h period.

Physical and chemical parameters

The flow of seawater in each flume was maintained at \sim 0.1 m s^{-1} using a pump (W. Lim Wave II 373 J s^{-1}). Flow speeds were measured across the working sections of the flumes using a Nortek Vectrino Acoustic Doppler Velocimeter, and the flow speed was selected to match representative flow speeds across the back reef of Moorea (Hench et al. 2008). The flumes received natural sunlight that was reduced with neutral density screening to light levels similar to those experienced at 2-m depth in the back reef (Carpenter 2016b). Maximum daily photosynthetically active radiation (PAR, 400–700 nm) typically ranged between 1000 and 2000 μmol quanta $\text{m}^{-2} \text{s}^{-1}$ (Fig. 1), with strong variation attributed to seasonal and daily weather. Temperatures in each flume were controlled individually with dedicated chillers, and were maintained to approximate the mean monthly seawater temperature in the back reef of Moorea. They were increased from \sim 27 °C in November to \sim 30 °C in March (Edmunds et al. 2010). Temperatures were ramped slowly (1 °C/month) between seasons.

Seawater carbonate chemistry was uncontrolled in one flume (ambient, \sim 344 μatm pCO_2) and controlled in the other three to simulate conditions arising from targeted pCO_2 values of 400, 1000 and 1300 μatm . The mean pCO_2 values achieved in these treatments were 344, 633, 870, and 1146, respectively. Treatments were selected to: (a) span the range of atmospheric pCO_2 values expected by the middle of the next century assuming a pessimistic scenario for anthropogenic effects (IPCC 2014), and (b) to facilitate an ANCOVA statistical approach, in which pCO_2

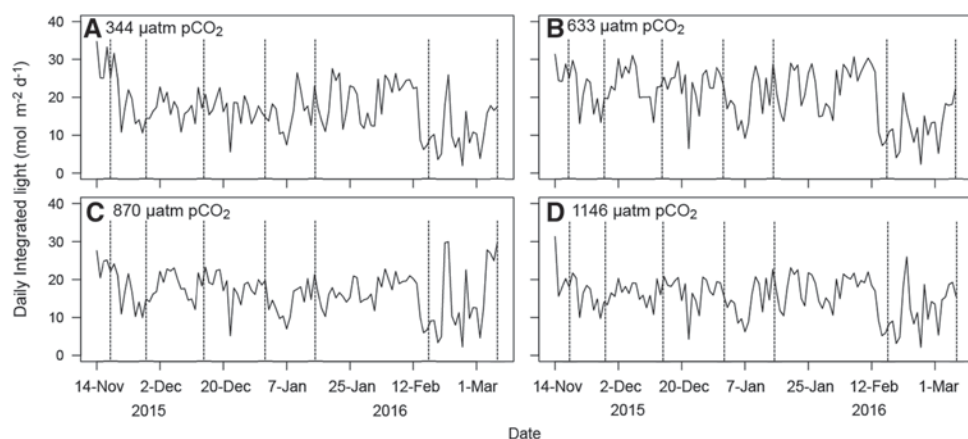


Fig. 1 Daily integrated PAR in each flume from 14 November 2015 to 15 March 2016 ($n=123$ days). PAR was measured with a cosine-corrected sensor recording at 0.6 mHz, and daily values were obtained by integrating records for each 24-h period. **a** Ambi-

ent flume (344 μatm pCO_2), **b** flume maintained at $\sim 633 \mu\text{atm}$ pCO_2 , **c** flume maintained at $\sim 870 \mu\text{atm}$ pCO_2 , and **d** flume maintained at $\sim 1146 \mu\text{atm}$ pCO_2 . Vertical dashed lines indicate dates on which metabolism measurements were made

was as a covariate, G_{net} and P_{net} were response variables, and time was a fixed effect. Seawater pH was not altered in the ambient flume, but was controlled in the treatment flumes (as a means to manipulate seawater pCO_2), with the bubbling pure CO_2 into the seawater. The desired pH set point (and corresponding pCO_2 set point) was maintained with the use of a pH-stat (Aquacontroller, Neptune systems, USA), which controlled the rate of bubbling of CO_2

through a solenoid which was opened when the attached pH electrode measured an increase in pH above the set point. A diurnal upward adjustment of ~ 0.1 pH unit was applied to the three treatment flumes to simulate current levels of diurnal variability in the back reef of Moorea (Hofmann et al. 2011); the ambient flume (which was not regulated for pCO_2) maintained a similar diel cycle with nighttime pH ~ 0.1 lower than daytime values (Table 1).

Table 1 Mean ($\pm \text{SE}$) of physical and chemical parameters measured/calculated in the flumes from 17 November 2015 to 15 March 2016

Treatment	Salinity	Temperature (°C)	pH_T	pCO_2 (μatm)	DIC ($\mu\text{mol kg}^{-1}$)	A_T ($\mu\text{mol kg}^{-1}$)	Ω_{ar}
344 μatm							
Overall	35.8 (†)	28.4 (†)	8.10 (§)	344 \pm 13	1949 \pm 10	2327 \pm 10	4.26 \pm 0.09
Day		28.6 (†)	8.14 (§)	305 \pm 11	1919 \pm 9	2325 \pm 7	4.56 \pm 0.10
Night		28.3 (†)	8.06 (§)	384 \pm 14	1979 \pm 14	2328 \pm 13	3.96 \pm 0.09
633 μatm							
Overall	35.8 (†)	28.3 (†)	7.88 (§)	633 \pm 23	2072 \pm 7	2319 \pm 8	2.92 \pm 0.06
Day		28.3 (†)	7.94 (§)	529 \pm 20	2035 \pm 8	2316 \pm 7	3.25 \pm 0.08
Night		28.2 (†)	7.82 (§)	737 \pm 29	2109 \pm 7	2323 \pm 11	2.58 \pm 0.06
870 μatm							
Overall	35.8 (†)	nd	7.76 (§)	870 \pm 14	2129 \pm 14	2315 \pm 18	2.31 \pm 0.05
Day		nd	7.80 (§)	771 \pm 12	2104 \pm 14	2309 \pm 16	2.50 \pm 0.04
Night		nd	7.72 (§)	968 \pm 25	2154 \pm 15	2320 \pm 20	2.13 \pm 0.06
1146 μatm							
Overall	35.8 (†)	28.4 (†)	7.66 (§)	1146 \pm 36	2195 \pm 6	2337 \pm 6	1.90 \pm 0.04
Day		28.4 (†)	7.68 (§)	1086 \pm 71	2182 \pm 11	2334 \pm 6	2.01 \pm 0.06
Night		28.4 (†)	7.64 (§)	1206 \pm 25	2208 \pm 7	2339 \pm 8	1.80 \pm 0.03

Seawater temperature was measured with Hobo temperature loggers whose values were averaged by day ($n=120$); salinity was measured weekly (17 days throughout the experiment) when seawater chemistry (pH_T , pCO_2 , DIC, A_T and Ω_{ar}) was analyzed (all $n=17$); multiple measurements for each day were averaged to produce diel (overall), day, or night values. Values of pCO_2 , DIC, and Ω_{ar} , were calculated from pH_T and A_T using Seacarb (Lavigne and Gattuso 2013)

SE ± 0.05 , ± 0.01 ; nd data lost due to sensor failure

Ambient air was bubbled continuously into all flumes (except during dissolved oxygen measurements) and there was no downward regulating of pCO_2 at night. We reasoned that the effects of nocturnal respiration in generating pCO_2 was a component of natural reef metabolism, and that extreme swings in pCO_2 due to this effect would be minimized by the constant in-flow of fresh seawater. Periodic measurements of nocturnal pCO_2 in the flumes confirmed that nocturnal pCO_2 exceeded daytime target values.

Throughout the experiment and in all flumes, logging sensors (sampling every 30 min) recorded PAR (using cosine-corrected PAR loggers, Dataflow Systems Ltd, Christchurch, New Zealand), and temperature [Hobo Pro v2 ($\pm 0.2^\circ\text{C}$), Onset Computer Corp., Bourne, MA]. pH, measured on the total hydrogen ion scale (pH_T), was monitored daily at the downstream end of the flumes with a handheld electrode (described below). Based on the values relative to target values, the thermostat and pH-stat set points were adjusted as necessary to maintain stable treatments. Seawater carbonate chemistry and salinity were measured weekly, both in the day (02:00) and night (20:00); salinity was measured using a bench-top conductivity meter (Thermo Scientific, Orionstar A212, Waltham, MA, USA). The parameters of the seawater carbonate system were calculated from measurements of temperature, salinity, pH_T , and A_T , using the R package seacarb (Lavigne andGattuso 2013). Calculations were made using the carbonic acid dissociation constants of Lueker et al. (2000), the K_{SO_4} concentration for the bisulfate ion from Dickson (1990), and the K_f constant of Perez and Fraga (1987).

pH_T was measured using a DG 115-SC electrode (Mettler-Toledo) that was calibrated with a TRIS buffer (SOP 6a Dickson et al. 2007). Total alkalinity was measured potentiometrically using the open-cell method of acidimetric titration (SOP 3b, Dickson et al. 2007) using certified acid titrant (from the Dickson lab) with a T50 Mettler-Toledo automatic titrator fitted with a DG 115-SC electrode (Mettler-Toledo). The accuracy and precision of these measurements were determined through analysis of certified reference materials (CRMs; from A. Dickson Laboratory, Scripps Institution of Oceanography). The mean ($\pm \text{SE}$) difference between measured and certified values (i.e., accuracy) was $1.7 \pm 0.3 \mu\text{mol kg}^{-1}$ ($n=15$) and the mean ($\pm \text{SE}$) precision of A_T analyses based on duplicate samples was $1.8 \pm 0.1 \mu\text{mol kg}^{-1}$ ($n=475$).

Community metabolism

Community G_{net} and P_{net} for the reef communities in the flumes initially were measured under ambient seawater carbonate chemistry conditions on two occasions on 14 and 16 November, 2015. The pCO_2 treatments then were initiated (on 17 November 2015), and community G_{net} and P_{net} were measured on 17–18 November 2015. Thereafter, community

G_{net} and P_{net} were measured biweekly or monthly until March 2016.

Community G_{net} was measured using the alkalinity anomaly method (Eq. 1, after Smith (1973)), and community P_{net} was measured using changes in dissolved oxygen (DO) (Eq. 2):

$$G_{\text{net}} = \frac{-0.5\Delta A_T V \rho}{\Delta t \text{SA}} \quad (1)$$

$$P_{\text{net}} = \frac{\Delta \text{DO} V \rho}{\Delta t \text{SA}}, \quad (2)$$

where ΔA_T is the change in total alkalinity ($\mu\text{mol kg}^{-1}$), V is the volume of seawater in the flumes (L), ρ is the density of the seawater (kg L^{-1}), Δt is the time interval of the incubations (h), SA is the planar area of the floor of the working area of the flumes (m^2), and ΔDO is the change in dissolved oxygen concentration over the incubation time ($\mu\text{mol kg}^{-1} \text{h}^{-1}$).

The addition of fresh seawater into the flumes was halted during each measurement of community P_{net} and G_{net} , so that changes in A_T and dissolved oxygen (DO) for the fixed volume of water within the flumes could be used to calculate P_{net} and G_{net} . Circulation of seawater within the flumes was maintained at a constant velocity (0.1 m s^{-1}) throughout the measurement period. The exchange of O_2 across the air–seawater interface at the surface of the flumes was assumed to be negligible during the incubations based on the rationale that UV-transparent acrylic covers that were placed over the flumes to prevent access by rain, and also greatly reduced wind movement at the seawater surface in the flumes. Incubations were designed to be implemented with four consecutive measurements of P_{net} and G_{net} in each flume during the day, with each incubation lasting ~ 3 h, and two determinations of respiration (R) and G_{net} at night, with each incubation lasting ~ 6 h. This protocol was consistent with our previous work (Comeau et al. Comeau et al. 2014a, b; 2015), but during the 4-month experiment, logistical constraints resulted in slight departures from this design, in the number of replicates during the day and night, incubation duration, and the start and end of incubations relative to sunrise and sunset. Between incubations within a measurement day, flumes were flushed with seawater for ~ 30 min at 5 L min^{-1} , which ensured that 25–30% of the seawater within each flume was replaced before the next incubation began. A_T was measured at the start and end of each incubation as described above, and DO was recorded each minute with MiniDOT DO loggers (Precision Measurement Engineering, Inc., Vista, CA, USA). DO sensors were calibrated by the manufacturer.

Measurements of community G_{net} and P_{net} over 3-h periods for daytime ($n=4$) and 6-h periods for nighttime ($n=2$)

were averaged, and used to estimate daily community G_{net} (over 24 h) and daytime community P_{net} (over ~ 12 h). As G_{net} and P_{net} predictably vary through the day, missing values from the set of six possible daily incubations biased the daily averages. To adjust for this effect, missing values were replaced with values calculated by interpolation using empirical, best-fit relationships of mean hourly G_{net} and P_{net} against time for each treatment. Third-order polynomials were used to describe the relationships between G_{net} and time, and fourth-order polynomials were used to describe the relationships between P_{net} and time (described in results). Daytime community G_{net} and P_{net} were calculated from the mean of the four, ~ 3 -h incubations during the day, and scaled to the mean local day length by month: 12.93 h in November 2015, 13.15 h in December 2015, 12.03 h in January 2016, 12.63 h in February 2016, and 12.17 h in March 2016. Nighttime community G_{net} was calculated from the mean of the two, 6-h night incubations scaled to the length of the night. Daily (24 h) values of G_{net} were derived from the sum of the day and night rates, and P_{net} was calculated only for daytime.

Statistical analyses

To test the hypothesis that daily community G_{net} and P_{net} varied among treatments over 4 months, ANCOVA was used where pCO_2 was the covariate, and time (sampling periods) was a fixed effect. The assumption of linearity for each treatment was tested using linear regressions, and an effect of time was detected as differences in slopes or elevations (intercepts) among incubations. Post hoc tests of levels within main effects were conducted using Tukey's HSD. To evaluate the role of P_{net} in modulating G_{net} on a scale of hours, the association between hourly P_{net} and G_{net} for each treatment was tested with Pearson correlations. Where these associations were significant, best-fit linear regressions were fit by Model I techniques, because the purpose was prediction of G_{net} from P_{net} (Sokal and Rohlf 2012). Pearson correlation also was used to test for an association between G_{net} and Ω_{ar} , and the predictive relationship between the two was described with Model I linear regression. Statistical analyses were performed using Systat 13 software, and statistical assumptions of ANCOVA (normality and equal variances) were tested using graphical analyses of residuals.

Results

Physical and chemical conditions

Seawater temperature, salinity, and carbonate chemistry for each flume are reported in Table 1, and are separated by day, night, and each 24 h day. The temperature logger in one

flume (870 μatm) failed and continuous records from this flume were lost. Spot measurements with a handheld meter showed that the temperature of this flume closely tracked the temperature of the other three flumes. Seawater temperature was similar among the three flumes with continuous records, and in all cases the mean daily temperatures were ~ 28.4 °C (Table 1). Seawater temperature in the flumes varied slightly throughout each day, with solar warming and nocturnal cooling, so that mean daytime temperatures were up to 0.3 °C higher than mean nighttime temperatures (Table 1). Temperature in the flumes tracked seasonal warming throughout the austral summer, and increased from ~ 27.5 °C in November to ~ 29.0 °C in March at ~ 0.014 °C day $^{-1}$ ($r^2=0.790$).

Salinity was consistent at 35.8 ± 0.1 psu among flumes throughout the experiment (Table 1). PAR varied among days in response to local weather (Fig. 1), and while it did not vary strikingly throughout the summer, it was reduced by clouds and rain in February and March 2016. Mean daily integrated PAR was 17.1 ± 0.6 mol quanta m^{-2} day $^{-1}$ in the 344 μatm pCO_2 flume, 20.1 ± 0.6 mol quanta m^{-2} s $^{-1}$ in the 633 μatm pCO_2 flume, 15.8 ± 0.5 mol quanta m^{-2} s $^{-1}$ in the 870 μatm pCO_2 flume, and 16.9 ± 0.6 mol quanta m^{-2} day $^{-1}$ in the 1146 μatm pCO_2 flume (\pm SE, $n=120$). PAR differed among flumes ($F=10.990$, $df=3$, 476, $P<0.001$) and was higher in the 633 μatm flume compared to the other flumes (Scheffé post hoc, $P\leq 0.001$). Variation in PAR between flumes arose from variable shading from the structure supporting the shade cloth above the flumes. A_T of seawater was similar among flumes, with mean daily values ranging from 2315 to 2362 $\mu\text{mol kg}^{-1}$ (Table 1), and mean daytime values $\leq 0.3\%$ lower than mean nighttime values (Table 1). Actual pCO_2 treatments departed from targeted values, with discrepancies strongest during the day and smallest at night (Table 1). pCO_2 differed among flumes for daily, daytime, or nighttime values ($F\geq 12.879$, $df=1.66$, $P\leq 0.001$); actual treatments contrasted mean pCO_2 values of 344, 633, 870 and 1146 μatm , which corresponded to mean Ω_{ar} values of 4.26, 2.92, 2.31, and 1.90, respectively (Table 1).

Community metabolism prior to pCO_2 treatments

Prior to establishing pCO_2 treatments in the flumes (i.e., ~ 344 μatm pCO_2), mean (\pm SD) daily G_{net} ($n=2$ days) was similar among flumes, ranging from 85 ± 18 to 92 ± 5 $\text{mmol CaCO}_3 \text{ m}^{-2} \text{ day}^{-1}$ (Fig. 2). Mean (\pm SD) daytime P_{net} was more variable among flumes, ranging from 42 ± 3 (344 μatm pCO_2 flume) to 60 ± 3 $\text{mmol O}_2 \text{ m}^{-2} \text{ day}^{-1}$ (1146 μatm pCO_2 flume) (Fig. 2).

Diel patterns of G_{net} and P_{net}

Hourly community G_{net} and P_{net} showed consistent diel responses, increasing during the morning to maxima near

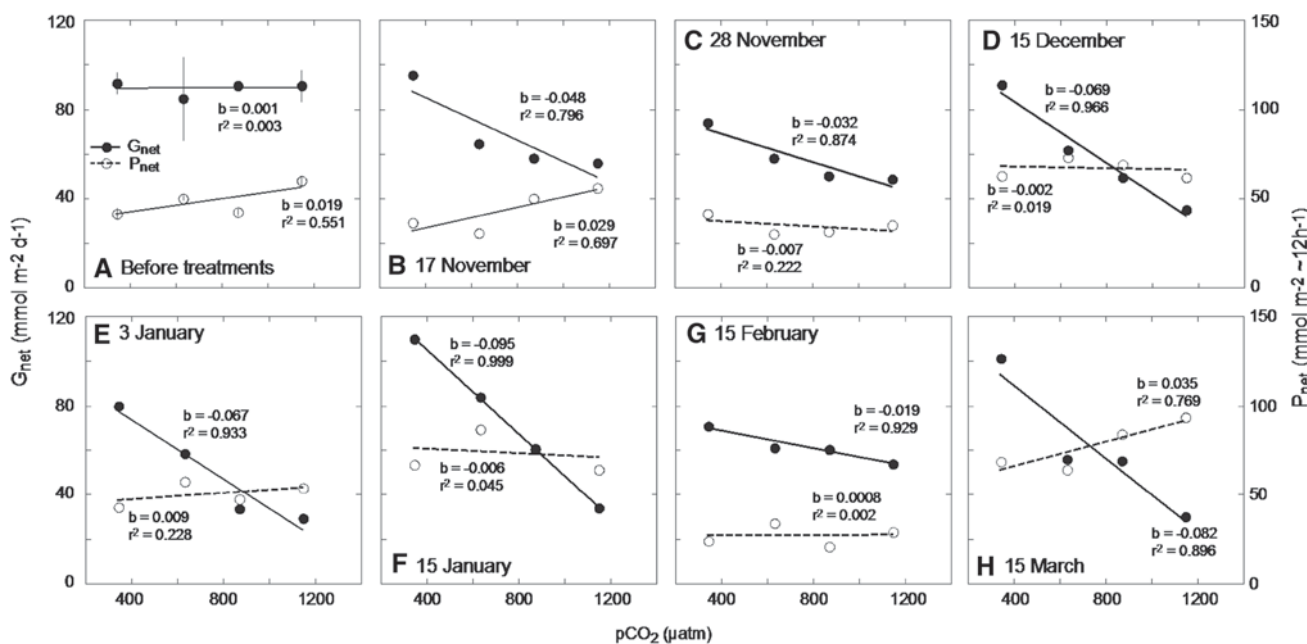
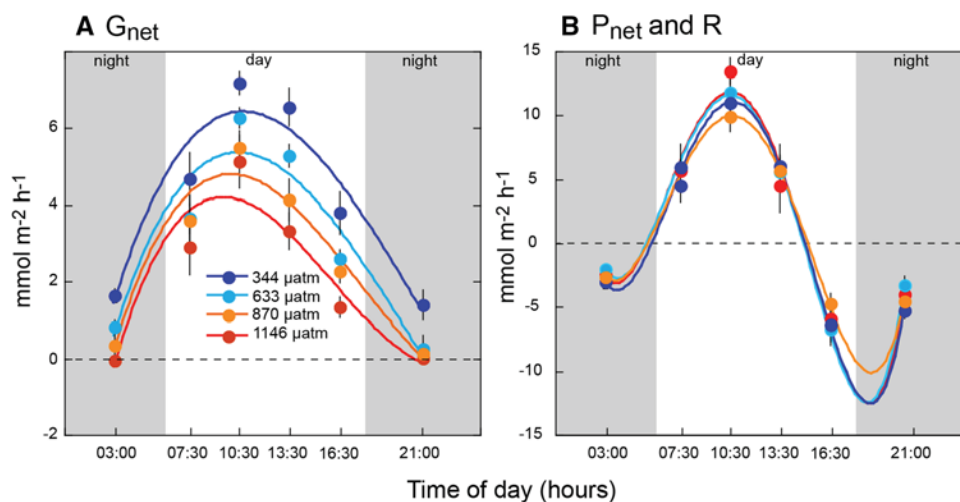


Fig. 2 Community net calcification (G_{net}) and primary productivity (P_{net}) of reef communities assembled in four flumes and incubated for 4 months at pCO_2 values of $\sim 344 \mu\text{atm}$ (ambient), $\sim 633 \mu\text{atm}$ pCO_2 , $\sim 870 \mu\text{atm}$ pCO_2 , and $\sim 1146 \mu\text{atm}$ pCO_2 (Table 1). **a** Values before pCO_2 treatments were initiated ($n=2, \pm \text{SD}$), **b** 17 November, **c** 28 November, **d** 15 December, **e** 3 January 2016, **f** 15 January 2016, **g** 15 February 2016, and **h** 15 March 2016. Logistical constraints resulted in some lost incubations (G_{net} in flume 3 between 15:00 and

18:00 h on 15 December, G_{net} in all flumes between 15:00 and 18:00 on 15 January, P_{net} in all flumes between 09:00 and 12:00 h on 3 January, and between 15:00 and 18:00 h on 15 January), and these values were interpolated using the relationships shown in Fig. 3; there was only one night time incubation on 28 November, but this lasted ~ 11 h. Lines are best-fit Model I regressions with slopes (b) and proportion of variance explained (r^2) reported

Fig. 3 Hourly G_{net} , P_{net} and R for the four flumes operated with pCO_2 treatments from 17 November 2015 to 15 March 2016. Values are mean ($\pm \text{SE}$) of all determinations and are plotted against the mid point of the intervals the incubations targeted for sampling (00:00–06:00, 06:00–09:00, 09:00–12:00, 12:00–15:00, 15:00–18:00, and 18:00–24:00). Curves are third-order polynomials for G_{net} ($r^2 \geq 0.899$), and fourth-order polynomials for P_{net} and R ($r^2 \geq 0.976$). $n=6$ –7 for G_{net} and 5–7 for P_{net} and R



the solar zenith and decreasing throughout the afternoon (Fig. 3). To describe the shape of these relationships and develop predictive capacity for G_{net} and P_{net} as a function of time of day, the data were fitted with third- or fourth-order polynomials. The use of these relationships is not intended to imply any explicit type of functional relationship. For G_{net} , the relationships with median incubation time were well fit by third-order polynomials ($r^2 \geq 0.900$),

and while the shapes of the responses were similar across treatments, maximum values differed among flumes, with the highest value under ambient pCO_2 , and lowest under the highest pCO_2 (Fig. 3). For P_{net} , the relationships with median incubation times were well fit with fourth-order polynomials ($r^2 \geq 0.976$), but for this dependent variable, the shapes of the relationships and the maximum values of P_{net} were very similar across treatments. The overall shape

of the diel response curve for community G_{net} was broader than for community P_{net} , with G_{net} increasing earlier in the day and maintaining positive values later in the day, while P_{net} increased and decreased steeply on either side of the solar zenith and was negative both early and late in the day, reflecting respiration.

Effect of treatment duration on net community calcification

Following initiation of the pCO_2 treatments, the responses of the communities were measured on 17/18 November (time = 1 day), 28 November (time = 12 days), 15/16 December (time = 29 days), 3/4 January (time = 48 days), 15/16 January (time = 60 days), 15/16 February (time = 91 days), and 15/16 March (time = 120 days). During these periods, in the 344 μatm flume, hourly G_{net} ranged from -0.47 to $8.37 \text{ mmol m}^{-2} \text{ h}^{-1}$, and hourly P_{net} from -10.67 to $13.97 \text{ mmol m}^{-2} \text{ h}^{-1}$. In the 633 μatm flume, hourly G_{net} ranged from -1.63 to $7.36 \text{ mmol m}^{-2} \text{ h}^{-1}$, and hourly P_{net} from -11.76 to $16.66 \text{ mmol m}^{-2} \text{ h}^{-1}$. In the 870 μatm flume, hourly G_{net} ranged from -0.86 to $7.45 \text{ mmol m}^{-2} \text{ h}^{-1}$, and hourly P_{net} from -7.07 to $12.75 \text{ mmol m}^{-2} \text{ h}^{-1}$. In the 1146 μatm flume, hourly G_{net} ranged from -0.53 to $7.31 \text{ mmol m}^{-2} \text{ h}^{-1}$, and hourly P_{net} from -8.79 to $16.40 \text{ mmol m}^{-2} \text{ h}^{-1}$. Hourly G_{net} and P_{net} calculated from all of the incubations conducted in the day and the night were

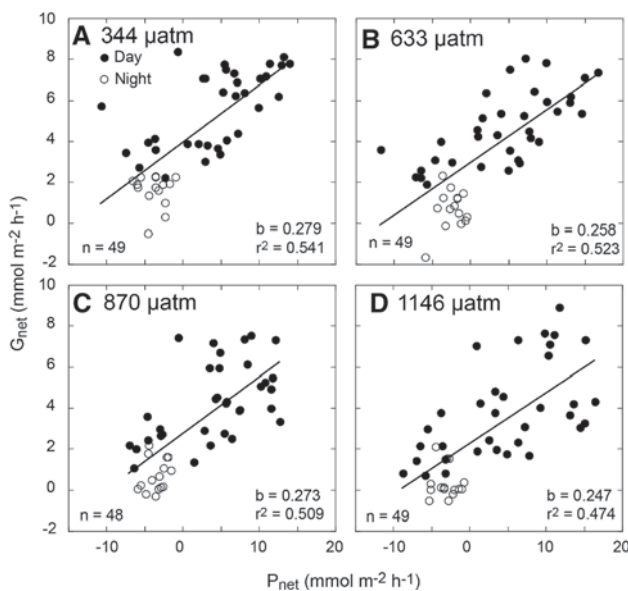


Fig. 4 Relationships between hourly coral reef community G_{net} and P_{net} for incubations completed in the day (filled circles) and the night (open circles) over the 4-month experiment. **a** 344 μatm pCO_2 flume, **b** 633 μatm pCO_2 flume, **c** 870 μatm pCO_2 flume, and **d** 1146 μatm pCO_2 flume. Lines are best-fit Model I regressions with their slopes (b), the proportion of variance explained (r^2) and sample size (n) shown

positively correlated in all four flumes (Fig. 4) ($r \geq 0.689$, $df = 48-48$, $P < 0.001$). Results from factorial ANCOVA indicated that the slopes of these relationships were similar between treatments ($b = 0.247-0.279$), but they differed in elevation and were depressed by high pCO_2 .

Over the 4-month period, community metabolism in the flumes was measured seven times under treatment conditions. During these measurements, logistical constraints resulted in five missing G_{net} values (18% of planned measurements), and one of the paired nighttime values was replaced with a single determination over ~ 12 h when the intermediate 6 h measured was omitted. Likewise, there were eight missing P_{net} values (29% of planned measurements). Missing values were interpolated using best-fit polynomial relationships for each flume (described above and in Fig. 3), and the complete set of measurements (empirical plus interpolated values) were used to calculate daily community G_{net} and P_{net} (Fig. 2b-h). Daily community G_{net} was negatively correlated with pCO_2 on four of seven sampling periods (with strong trends for two additional periods, Fig. 2,

Table 2 Results of least squares linear regression analysis (Model I) of daily community G_{net} and P_{net} against flume treatments (pCO_2) for seven periods (Time) over which treatments were sustained (Fig. 3)

Variable	Time	<i>F</i>	<i>df</i>	<i>P</i>	Slope
G_{net}	17 November 2015	7.805	1.2	0.108	n/a
	28 November 2015	13.935	1.2	0.069	-0.032 ± 0.009
	15 December 2015	57.145	1.2	0.017	-0.069 ± 0.009
	3 January 2016	28.442	1.2	0.033	-0.067 ± 0.012
	15 January 2016	4219.793	1.2	< 0.001	-0.095 ± 0.001
	15 February 2016	26.634	1.2	0.036	-0.020 ± 0.004
	15 March 2016	17.247	1.2	0.053	-0.082 ± 0.020
	17 November 2015	4.618	1.2	0.165	n/a
	28 November 2015	0.572	1.2	0.528	n/a
	15 December 2015	0.039	1.2	0.862	n/a
P_{net}	3 January 2016	0.588	1.2	0.523	n/a
	15 January 2016	0.095	1.2	0.787	n/a
	15 February 2016	0.005	1.2	0.950	n/a
	15 March 2016	6.690	1.2	0.123	n/a

F values, degrees of freedom (*df*), and slope of the relationships are shown (in units of $\text{mmol m}^{-2} \text{ day}^{-1} \mu\text{atm} \text{ pCO}_2^{-1}$) for relationships that either are significant ($P < 0.05$), or for which a trend is present ($P < 0.10$)

n/a not applicable (as $P \geq 0.107$)

Table 2). On 17 November, G_{net} was unaffected by pCO_2 , on 28 November, there was a trend ($P=0.069$) for G_{net} to decline with increasing pCO_2 , G_{net} declined ($P\leq 0.036$) with increasing pCO_2 on 15 December, 3 January, 15 January, and 15 February, and again there was a trend ($P=0.053$) for G_{net} to decline with pCO_2 on 15 March (Table 2). For the periods when G_{net} declined with increasing pCO_2 , the slopes of these relationships ranged from $-0.020\pm 0.004 \text{ mmol m}^{-2} \text{ day}^{-1} \mu\text{atm pCO}_2^{-1}$ to $-0.095\pm 0.001 \text{ mmol m}^{-2} \text{ day}^{-1} \mu\text{atm pCO}_2^{-1}$. In contrast to community G_{net} , community P_{net} was unaffected by pCO_2 for any of the seven sampling times when it was measured (Fig. 2, Table 2).

For the relationships between community G_{net} and pCO_2 , a contrast of the four significant relationships demonstrated that the slopes were heterogeneous ($F=15.262$, $df=3.8$, $P=0.001$), with the relationships on 15 January relatively steeper than 15 December ($P=0.022$), and 3 January ($P=0.001$), and the relationship on 3 January relatively steeper than on 15 February ($P=0.039$); no other contrasts were significant ($P\geq 0.057$). Although a contrast of all seven regression lines of community G_{net} against pCO_2 must be treated with caution, since three of the lines are not significant (Table 2), the analysis nevertheless suggests that the slopes differ among times ($F=5.037$, $df=6.14$, $P=0.006$). Post hoc contrasts indicate that the slope of the relationship on 3 January is steeper than the slope on 18 November ($P=0.034$), but less steep than the slope on 15 January ($P=0.010$); no other contrasts were significant ($P\geq 0.141$).

When averaged over all measurement periods (17 November 2015 to 15 March 2016), daily community G_{net} was

associated positively with Ω_{ar} (Fig. 5) ($F=376.448$, $df=1.2$, $P=0.003$), such that G_{net} declined with decreasing Ω_{ar} . The proportional effect differed depending on the initial value of Ω_{ar} , but, for example, this relationship suggests that a unit decline in Ω_{ar} from 4.0 is associated with a 24% reduction in G_{net} , but a 45% reduction from a Ω_{ar} value of 3.0.

Discussion

The major questions addressed by this study were: (1) how are G_{net} and P_{net} of reef communities affected by a range of potential ocean acidification conditions (700–1300 μatm), (2) Does OA affect the relationships between community G_{net} and P_{net} , and (3) are community responses of G_{net} and P_{net} to ocean acidification consistent over an extended period of time (4 months)? Before the pCO_2 treatments were established, G_{net} and P_{net} were broadly similar among flumes (zero slopes across treatments), indicating that the communities that were assembled within them to be similar to one another, and to the back reef community of Moorea in 2013, also were similar to one another in terms of their community metabolism. This outcome was striking even though the flumes differed in light intensity and likely, in the composition of the infauna residing within the sediment. After treatments began, G_{net} responded quickly and negatively to elevated pCO_2 , with an approximate reduction of 70% in the highest pCO_2 treatment compared to the ambient pCO_2 at the conclusion of this experiment (a contrast between the extremes of our pCO_2 treatments). While comparisons among experiments might result from variation in the sensitivity of organismal physiology and/or variation in actively calcifying area, this reduction in G_{net} is consistent with results of previous experiments in which back reef communities similar to those studied here were exposed to ~ 1000 –1300 $\mu\text{atm pCO}_2$. Working with a nearly identical community in Moorea, Comeau et al. (2015), for example, started with community G_{net} under ambient pCO_2 conditions (ca. $76 \text{ mmol m}^{-2} \text{ day}^{-1}$) that was within the range of values recorded here for similar pCO_2 conditions (~ 70 –110 $\text{mmol m}^{-2} \text{ day}^{-1}$), but they described a 59% decrease in community G_{net} at 1318 versus 456 $\mu\text{atm pCO}_2$ over 8 weeks. Working with patch reef communities from Heron Island, Australia, Dove et al. (2013) reported a greater decrease in G_{net} for experimental reef communities maintained at different pCO_2 levels over 3 months, with net calcification declining from $\sim +3 \text{ g day}^{-1}$ at 405 $\mu\text{atm pCO}_2$ and 26.1°C , to $\sim -1.4 \text{ g day}^{-1}$ (i.e., dissolution occurred) at 1009 $\mu\text{atm pCO}_2$ and 30.2°C . The stronger negative effect of high pCO_2 in Dove et al. (2013) (versus our study, Fig. 2), most likely was due to their implementation of a broader test of future environmental conditions in which both pCO_2 and temperature were elevated. In our experiment, the effects of

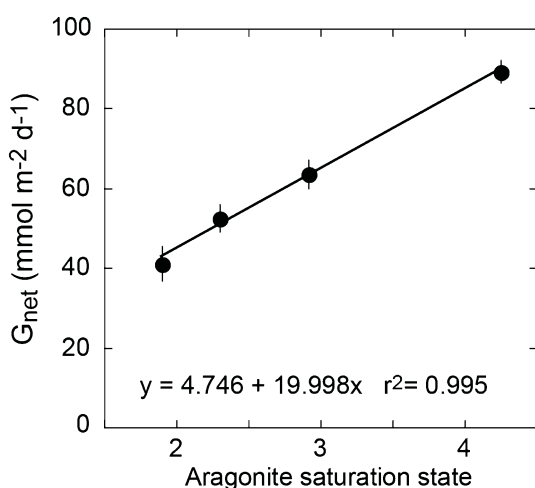


Fig. 5 Relationship between daily integrated community G_{net} and aragonite saturation state (Ω_{ar}) for each of the four experimental flumes maintained at a different pCO_2 . Values shown are mean \pm SE ($n=15$ for Ω_{ar} 4.25, all others, $n=7$). G_{net} and Ω_{ar} were associated significantly ($r=0.998$, $df=2$, $P=0.002$), and the line shows the Model I least squares linear regression that is used to describe the functional relationship between the variables

pCO₂ treatments on G_{net} also were evident on diurnal time scales, where G_{net} was reduced throughout the day with a consistent monotonic, negative relationship with pCO₂. G_{net} in all treatments increased rapidly in the morning, peaked at midday, and then gradually decreased in the afternoon and evening. One reason for this strong diurnal response is that it might reflect the requirements for, and the capacity to supply, the metabolic energy necessary to support higher rates of G_{net} , with the parsimonious source of this energy being community P_{net} earlier in the day. G_{net} was positive throughout the day and became negative during the night in all treatments.

There was no evidence that P_{net} was affected by high pCO₂. It appeared that P_{net} was more variable over time than between treatments, likely due to variation among measurement days in PAR. Several previous studies also have reported no effect of OA on P_{net} for coral reef communities (Leclercq et al. 2002; Langdon and Atkinson 2005; Dove et al. 2013; Comeau et al. 2015). These results suggest that photosynthesis of coral reef primary producers is not “fertilized” by the additional CO₂ and HCO₃ available under reduced seawater pH conditions, at least over the time scales of our measurements (but see e.g., Noonan and Fabricius 2016). There was a consistent and positive relationship between P_{net} and G_{net} expressed on an hourly basis. Generally, it is presumed that photosynthesis stimulates G_{net} in at least two ways. First, photosynthesis produces energy (ATP) and compounds that can be used to support calcification, either to fuel calcium uptake, proton pumping (Comeau et al. 2017), and/or the construction of an organic matrix on which calcium carbonate is laid down (Allemand et al. 2011; Tambutte et al. 2011). Additionally, photosynthesis elevates the local pH, which can create chemical conditions that facilitate calcification (Comeau et al. 2017). As a result, on hourly time scales, P_{net} may drive G_{net} directly. Since P_{net} is closely coupled with PAR, G_{net} too will be driven (indirectly) by PAR, although the effect of PAR on P_{net} and G_{net} is evident only on short time scales (hours), and is unlikely to appear over daily periods (i.e., involving the integrated effects of PAR). This suggest that the coupling between P_{net} and G_{net} is related to processes occurring over short time scales (e.g., energy production, pH alteration), rather than the overall balance between the long-term demands for metabolic energy and the capacity to supply it through the catabolism of short- and long-term food reserves, all of which create time lags in the hysteresis pattern between G_{net} and PAR.

The relationships between G_{net} and P_{net} were not affected by the pCO₂ treatments, as the slopes of these relationships did not differ. The slope of G_{net} regressed on P_{net} for coral reefs typically are related to the composition of the benthic community (Page et al. 2016), with higher values for communities dominated by calcifying taxa, and lower values for communities dominated by fleshy

macroalgae (Lantz et al. 2014). The values of the $G_{\text{net}}/P_{\text{net}}$ slopes [unit-less and often given as NEC/NEP (e.g., Shaw et al. 2015)] in the present study (0.247–0.279) are within the range of those reported for other coral reefs having a community structure of scleractinians and algae similar to that employed herein (Suzuki and Kawahata 2003). The elevations of these relationships, however, were affected by pCO₂ and were increasingly lower, as pCO₂ increased from 344 to 1146 μatm .

Because our experimental reefs contained a combination of calcifying and non-calcifying organisms together with reef sediments, the responses of community G_{net} to pCO₂ reflects the combined effect of elevated pCO₂ on organismal calcification, dissolution of organism carbonate skeletons, and abiotic calcification/dissolution of inorganic carbonate sediments (Eyre et al. 2014). Results from mesocosm experiments on the effects of OA on organismal G_{net} for several coral and calcified algal species suggest that the effects of elevated pCO₂ are variable, but generally negative (Chan and Connolly 2013; Kroeker et al. 2013; Comeau et al. 2014a, b), and this reduction in organism G_{net} is a combination of reduced calcification, enhanced bioerosion, and skeletal dissolution. In a very similar experiment to that reported here, ~50% of the reduction in community G_{net} under elevated pCO₂ was due to dissolution of sediments, mostly at night (Comeau et al. 2015). For this reason, extrapolation of OA effects from organism-scale experiments to the community scale are problematic, and the important role of sediments needs to be incorporated when attempting to predict responses at the reef scale (Eyre et al. 2014; Edmunds et al. 2016). This may be less problematic on coral reefs with a relatively low diversity of benthic calcifiers where net calcification of component taxa and functional groups can be scaled with a high degree of accuracy to estimate net community calcification (Courtney et al. 2016).

To date, little is known about the extended effects (i.e., over months or years) of OA on organism or community primary production or calcification (Kroeker et al. 2013). To test hypotheses regarding these effects, we established a multi-month OA experiment to examine whether OA effects on G_{net} and P_{net} are time-dependent. With our results to date, and based on previous experiments, we can evaluate the support for three alternative hypotheses with respect to how OA effects are manifested through time. The first hypothesis (the null) is that the slopes of community G_{net} and P_{net} as a function of pCO₂ are negative and do not change over time. This would indicate that OA effects on reef metabolism are negative (based on prior results) and constant. A second hypothesis is that the slopes of community G_{net} and P_{net} with pCO₂ increase over time, indicating that OA effects are cumulative and have additive (or multiplicative) effects. A third alternative hypothesis is that slopes of community G_{net} and P_{net} with pCO₂ are negative, but the slope of the

relationships became less steep over time. This could be construed as evidence of acclimatization of organisms in the community to OA, and/or amelioration of negative effects by longer-term community processes (e.g., sediment dissolution and local increases in buffering capacity).

For the first hypothesis, the community P_{net} was unaffected by pCO_2 , and thus, the slope of P_{net} on pCO_2 was zero initially, and did not change over 4 months. This result is consistent with previous studies, based on which a recent meta-analysis concluded that photosynthesis in a variety of tropical marine taxa (corals, coccolithophores, fleshy macroalgae, and seagrasses) was unaffected by OA over any of the time scales tested (Kroeker et al. 2013). In the test of the second hypothesis, our results for the response of G_{net} to pCO_2 were very different, however, for while G_{net} did not vary among flumes at the start of the experiment (i.e., before treatments were applied), it was strongly affected by pCO_2 throughout the study, with $G_{\text{net}}\text{-pCO}_2$ slopes differing among the months. The steepest slopes were recorded on 15 January and 15 March, the shallowest slopes on 28 November and 15 February, and the seven samplings created a ranking of sensitivities of G_{net} to pCO_2 of 16 January > 15 March > 15 December > 3 January > 17 November > 28 November > 15 February. This ranking does not conform well to any of our three a priori hypotheses (described above), although the responses consistently were negative (an outcome encapsulated in our first alternative hypothesis). Critically, our results support neither an intensifying (H_a 2 above) nor an attenuating (our H_a 3 above) model of coral community sensitivity of G_{net} and P_{net} to pCO_2 over time scales as long as 4 months. However, the labile response of the $G_{\text{net}}\text{-pCO}_2$ relationship of Moorea back reef communities suggests their net calcification is sensitive to seasonally varying environmental conditions. In this regard, the day-to-day, monthly, and seasonal variation in integrated PAR (Fig. 1) in the flumes is high, and it appears that the lowest sensitivity of G_{net} to pCO_2 was coincident with weather patterns that reduced PAR through clouds and rain (i.e., in late November and middle February). Likewise, the greatest sensitivity of G_{net} to pCO_2 was coincident with high PAR in the middle of January, December, and March. These patterns of variation in the sensitivity of G_{net} to pCO_2 , and the inferred association with PAR, are consistent with past results at the organismal level for tropical scleractinian corals and calcified algae. Critically, our previous work suggest that calcifying organisms that are calcifying at high rates, for example, as occurs under high PAR, are the most sensitive to OA (Comeau et al. 2014a), and the present study suggests a similar relationship may extend to reef communities and affect G_{net} .

In summary, the results of this experiment begin to provide temporal rigor to the emerging understanding of the effects of OA on coral reef organisms and the communities they build, specifically by extending the duration of exposure

to predicted future seawater conditions to 4 months. Relative to the effects of OA on coral reefs that already have been measured, our results provide more nuanced answers to the three questions at the core of this study. First, we demonstrate that G_{net} of an experimental back reef community was related negatively to pCO_2 over a four-month period, while community P_{net} was unaffected by the same treatments (Fig. 2). Second, we show that the relationships between community G_{net} and P_{net} were not affected by treatment, although the elevations of these relationships were reduced progressively with increases in pCO_2 (Fig. 4). Finally, we show that the effect of elevated pCO_2 on community G_{net} consistently was negative over seven consecutive measures extending over the 4 months, with no evidence of increases or decreases in sensitivity (slope) with time (Fig. 4). However, the sensitivity of G_{net} to OA appeared to be modulated, at least in part, by variation in light. Overall, our results highlight the utility of using experimental reef communities under ecologically relevant environmental conditions to test hypotheses about the immediate and time-dependent effects of OA on coral reef function. Further work over longer time scales is warranted to explore the possibilities that longer-term effects of OA on reef communities are less striking than those arising from short-term, acute exposures, and moreover, if reef communities exhibit the ability to acclimate to OA conditions.

Acknowledgements Funding for this study was provided by the National Science Foundation grant OCE 14-15268, and benefitted from support through the Moorea Coral Reef LTER program (NSF OCE 12-36905) and gifts from the Gordon and Betty Moore Foundation. Research was completed under permits issued by the Haut-commissariat de la République en Polynésie Française (DRRT) (Protocole d'Accueil 2015–2016). We thank J. Manning, J. Bergman, S. Merolla, B. Shayka, S. Comeau, V. Moriarty, A. Siravo, D. Sternberg and S. Zimmerman for assistance with maintaining the flumes over 4 months. We also are grateful to three reviewers whose comments improved the manuscript. This is contribution number 268 of the CSUN Marine Biology Program.

Compliance with ethical standards

This study was funded by the National Science Foundation (grant OCE-1415268). All authors declare that they have no conflict of interest. All applicable international, national, and/or institutional guidelines for the care and use of animals were followed.

References

Albright R, Caldeira L, Hosfelt J, Kwiatkowski L, Maclare JK, Mason BM, Nebuchina Y, Ninokawa A, Pongratz J, Ricke KL, Rivlin T, Schneider K, Sesboüé M, Shamberger K, Silverman J, Wolfe K, Zhu K, Caldeira K (2016) Reversal of ocean acidification enhances net coral reef calcification. *Nature* 53:362–365

Allemand D, Tambutté E, Zoccola D, Tambutté S (2011) Coral calcification: cells to reef. In: Dubinsky Z, Stambler N (eds) *Coral reefs: an ecosystem in transition*. Springer, Heidelberg

Andersson AJ, Gledhill D (2013) Ocean acidification and coral reefs: effect on breakdown, dissolution, and net ecosystem calcification. *Ann Rev Mar Sci* 5:321–348

Anthony KRN, Kline DI, Diaz-Pulido G, Dove S, Hoegh-Guldberg O (2008a) Ocean acidification causes bleaching and productivity loss in coral reef builders. *Proc Natl Acad Sci* 105:17442–17446

Anthony KRN, Kleypas JA, Gattuso JP (2008b) Coral reefs modify their seawater carbon chemistry—implications for impacts of ocean acidification. *Glob Change Biol* 12:3655–3666

Atkinson MJ, Barnett H, Aceves H, Langdon C, Carpenter SJ, McCunnahay T, Hochberg E, Smith M, Marino BDV (1999) The Biosphere 2 coral reef biome. *Ecol Eng* 13:147–172. [https://doi.org/10.1016/S0925-8574\(98\)00096-2](https://doi.org/10.1016/S0925-8574(98)00096-2)

Carpenter R (2016a) MCR LTER: coral reef: long-term population and community dynamics: benthic algae and other community components. knb-lter-mcr.8.28 <https://doi.org/10.6073/pasta/79a6edbcf3aa2380d43deed778856416>

Carpenter R (2016b) MCR LTER: coral reef: benthic photosynthetically active radiation (PAR), ongoing since 2009. knb-lter-mcr.4005.8 <https://doi.org/10.6073/pasta/ea06e6d53df8b1c df7c1d50d025b77fd>

Chan NCS, Connolly SR (2013) Sensitivity of coral calcification to ocean acidification: a meta-analysis. *Glob Change Biol* 19:282–290

Comeau S, Atkinson MJ, Spindel NB, Carpenter R (2014a) Fast coral reef calcifiers are more sensitive to ocean acidification in short-term laboratory incubations. *Limnol Oceanogr* 59:1081–1091

Comeau S, Edmunds PJ, Lantz CA, Carpenter R (2014b) Water flow modulates the response of coral reef communities to ocean acidification. *Nat Sci Rep* 4:6681

Comeau S, Carpenter RC, Lantz CA, Edmunds PJ (2015) Ocean acidification accelerates dissolution of experimental coral reef communities. *Biogeosciences* 12:365–372

Comeau S, Lantz CA, Edmunds PJ, Carpenter RC (2016) Framework of barrier reefs threatened by ocean acidification. *Glob Change Biol* 22:1225–1234

Comeau S, Tambutté E, Carpenter RC, Edmunds PJ, Evensen NR, Allemand D, Ferrier-Pagès C, Tambutté S, Venn AA (2017) Coral calcifying fluid pH is modulated by seawater carbonate chemistry not solely seawater pH. *Proc R Soc B Biol Sci* 284:20161669. <https://doi.org/10.1098/rspb.2016.1669>

Courtney TA, Andersson AJ, Bates NR, Collins A, Cyronak T, de Putron SJ, Eyre BD, Garley R, Hochberg EJ, Johnson R, Musielewicz S, Noyes TJ, Sabine CL, Sutton AJ, Tonkin J, Tribollet A (2016) Comparing chemistry and census-based estimates of net ecosystem calcification on a rim reef in Bermuda. *Front Mar Sci* 3:181. <https://doi.org/10.3389/fmars.2016.00181>

Crawley A, Kline DI, Dunn S, Anthony K, Dove S (2010) The effect of ocean acidification on symbiont photorespiration and productivity in *Acropora formosa*. *Glob Change Biol* 16:851–863

DeCarlo TN, Cohen AL, Wong GTF, Shiah F-K, Lentz SJ, Davis KA, Shamberger KEF, Lohmann P (2017) Community production modulates coral reef pH and the sensitivity of ecosystem calcification to ocean acidification. *J Geophys Res* 122:745–761

Dennison WC, Barnes DJ (1988) Effect of water motion on coral photosynthesis and calcification. *J Exp Mar Biol Ecol* 115:67–77

Dickson AG, Wesolowski DJ, Palmer DA, Mesmer RE (1990) Dissociation constant of bisulfate ion in aqueous sodium chloride solutions to 250 °C. *J Phys Chem* 94:7978–7985. <https://doi.org/10.1021/j100383a042>

Dickson AG, CL Sabine, JR Christian (2007) Guide to best practices for ocean CO₂ measurements. North Pacific Marine Science Organization, Sidney, British Columbia, Canada

Doney SC, Fabry VJ, Feely RA, Kleypas JA (2009) Ocean acidification: the other CO₂ problem. *Ann Rev Mar Sci* 1:169–192

Dove S, Kline DI, Pantis S, Angly FE, Tyson GW, Hoegh-Guldberg O (2013) Future reef decalcification under a business-as-usual CO₂ emission scenario. *Proc Natl Acad Sci* 110:15342–15347

Edmunds P (2016) MCR LTER: coral reef: long-term population and community dynamics: corals. knb-lter-mcr.4.33. <https://doi.org/10.6073/pasta/1f05f1f52a2759dc096da9c24e88b1e8>

Edmunds PJ, Leichter JJ, Adjrououd M (2010) Landscape-scale variation in coral recruitment in Moorea, French Polynesia. *Mar Ecol Prog Ser* 414:75–89

Edmunds PJ, Comeau S, Lantz C, Andersson A, Briggs C, Cohen A, Gattuso JP, Grady JM, Gross K, Johnson M, Muller EB, Ries JR, Tambutté S, Tambutté E, Venn A, Carpenter RC (2016) Integrating the effects of ocean acidification across functional scales on tropical coral reefs. *Biosciences* 66:350–362

Eyre BD, Andersson AJ, Cyronak T (2014) Benthic coral reef calcium carbonate dissolution in an acidifying ocean. *Nat Clim Change* 4:969–976

Falter JL, Lowe RJ, Atkinson MJ, Monismith SG, Schar DW (2008) Continuous measurements of net production over a shallow reef community using a modified Eulerian approach. *J Geophys Res* 113:1–14

Falter JL, Lowe RJ, Atkinson MJ, Cuet P (2012) Seasonal coupling and de-coupling of net calcification rates from coral reef metabolism and carbonate chemistry at Ningaloo Reef, Australia. *J Geophys Res* 117:C05003

Frieder CA, Applebaum SL, Pan TCF, Hedgecock D, Manahan DT (2016) Metabolic cost of calcification in bivalve larvae under experimental ocean acidification. *ICES Mar Sci*. <https://doi.org/10.1093/icesjms/fsw213>

Gattuso JP, Pichon M, Delesalle B, Canon C, Frankignoulle M (1996) Carbon fluxes in coral reefs. I. Lagrangian measurement of community metabolism and resulting air-sea CO₂ disequilibrium. *Mar Ecol Prog Ser* 145:109–121

Hench JL, Leichter JL, Monismith SG (2008) Episodic circulation and exchange in a wave-driven coral reef and lagoon system. *Limnol Oceanogr* 53:2681–2694

Hoegh-Guldberg O, Mumby PJ, Hooten AJ, Steneck RS, Greenfield P, Gomez E, Harvell CD, Sale PF, Edwards AJ, Caldeira K, Knowlton N, Eakin CM, Iglesias-Prieto R, Muthiga N, Bradbury RH, Dubi A, Hatziolos ME (2007) Coral reefs under rapid climate change and ocean acidification. *Science* 318:1737–1742

Hofmann GE, Smith JE, Johnson KS et al (2011) High-frequency dynamics of ocean pH: a multi-ecosystem comparison. *PLoS One* 6:e28983

IPCC, 2014: Climate Change 2014: Synthesis Report. Contribution of Working Groups I, II and III to the Fifth Assessment Report of the Intergovernmental Panel on Climate Change [Core Writing Team, R.K. Pachauri and L.A. Meyer (eds.)]. IPCC, Geneva, Switzerland

Jones CG, Lawton JH, Shachak M (1994) Organisms as ecosystem engineers. *Oikos* 69:373–386

Kinsey DW (1978) Alkalinity changes and coral reef calcification. *Limnol Oceanogr* 23:989–991

Kinsey DW (1985) Metabolism, calcification and carbon production 1: system level studies. In: Proc 5th Int Coral Reef Congr, Tahiti 4:505–526

Kleypas JA, Yates KK (2009) Coral reefs and ocean acidification. *Oceanography* 22:108–117

Kroeker KJ, Kordas RL, Crim R, Hendriks IE, Ramajo L, Singh GS, Duarte CM, Gattuso JP (2013) Impacts of ocean acidification on marine organisms: quantifying sensitivities and interaction with warming. *Glob Change Biol* 19:1884–1896

Langdon C, MJ Atkinson (2005) Effect of elevated pCO₂ on photosynthesis and calcification of corals and interactions with seasonal

change in temperature/irradiance and nutrient enrichment. *J Geophys Res Oceans* 110:C09S07 1–C09S07 16

Lantz CA, Atkinson MJ, Winn CW, Kahng SE (2014) Dissolved inorganic carbon and total alkalinity of a Hawaiian fringing reef: chemical techniques for monitoring the effects of ocean acidification on coral reefs. *Coral Reefs* 33:105–115

Lavigne H, JP Gattuso (2013) Seacarb, seawater carbonate chemistry with R. R package version 2. 4. 10. Available at: <https://CRAN.R-project.org/package=seacarb> (accessed 11 July 2014).

Leclercq N, Gattuso JP, Jaubert J (2002) Primary production, respiration, and calcification of a coral reef mesocosm under increased CO_2 partial pressure. *Limnol Oceanogr* 47:558–564. <https://doi.org/10.4319/lo.2002.47.2.00558>

Lueker TJ, Dickson AG, Keeling CD (2000) Ocean pCO_2 calculated from dissolved inorganic carbon, alkalinity, and equations for K-1 and K-2: validation based on laboratory measurements of CO_2 in gas and seawater at equilibrium. *Mar Chem* 70:105–119

Noonan SHC, Fabricius KE (2016) Ocean acidification affects productivity but not the severity of thermal bleaching in some tropical corals. *ICES J Mar Sci* 73:715–726. <https://doi.org/10.1093/icesjms/fsv127>

Ohde S, van Woesik R (1999) Carbon dioxide flux and metabolic processes of a coral reef, Okinawa. *Bull Mar Sci* 65:559–576

Page HN, Andersson AJ, Jokiel PL, Rodgers KS, Lebrato M, Yeakel K et al (2016) Differential modification of seawater carbonate chemistry by major coral reef benthic communities. *Coral Reefs* 35:1–15. <https://doi.org/10.1007/s00338-016-1490-4>

Pandolfi JM, Connolly SR, Marshall DJ, Cohen AL (2011) Projecting coral reef futures under global warming and ocean acidification. *Science* 333:418–422

Perez FF, Fraga F (1987) Association constant of fluoride and hydrogen ions in seawater. *Mar Chem* 21:161–168

Perry CT, Murphy GN, Kench PS, Smithers SG, Edinger EN, Steneck RS, Mumby PJ (2013) Caribbean-wide decline in carbonate production threatens coral reef growth. *Nat Commun* 4:1402

Shaw EC, McNeil BI, Tilbrook B (2012) Impacts of ocean acidification in naturally variable coral reef flat ecosystems. *J Geophys Res Oceans* 117:C03038

Shaw EC, Phinn SR, Tilbrook B, Steven A (2015) Natural in situ relationships suggest coral reef calcium carbonate production will decline with ocean acidification. *Limnol Oceanogr* 60:777–788

Silverman J, Lazar B, Cao L, Caldeira K, Erez J (2009) Coral reefs may start dissolving when atmospheric CO_2 doubles. *Geophys Res Lett* 36:L05606. <https://doi.org/10.1029/2008gl036282>

Smith SV (1973) Carbon dioxide dynamics: a record of organic carbon production, respiration, and calcification in the Eniwetok reef flat community. *Limnol Oceanogr* 18:106–120

Smith SV, Kinsey DW (1978) Calcification and organic carbon metabolism as indicated by carbon dioxide. In: Stoddart DR, Johannes RE (eds) *Coral reefs: research methods*. UNESCO, Paris, pp 439–468

Sokal RR, Rohlf FJ (2012) *Biometry*, 4th edn. WH Freeman and Co., New York

Suzuki A, Kawahata H (2003) Carbon budget of coral reef systems: an overview of observations in fringing reefs, barrier reefs and atolls in the Indo-Pacific regions. *Tellus Ser B Chem Phys Meteorol* 55:428–444. <https://doi.org/10.1034/j.1600-0889.2003.01442.x>

Tambutte S, Holcomb M, Ferrier-Pages C, Reynaud S, Tambutte E, Zoccola D, Allemand D (2011) Coral biomineralization: from the gene to the environment. *J Exp Mar Bio Ecol* 408:58–78

Wild C, Hoegh-Guldberg O, Naumann MS, Colombo-Pallotta MF, Ateweberhan M, Fitt WK, Iglesisa-Prieto R, Palmer C, Bythell JC, Ortiz J-C, Loya Y, van Woesik R (2011) Climate change impedes scleractinian corals as primary reef ecosystem engineers. *Mar Freshw Res* 62:205–215